© 2021. Published by The Company of Biologists Ltd | Journal of Cell Science (2021) 134, jcs256230. doi:10.1242/jcs.256230

RESEARCH ARTICLE

Interferon regulatory factor 7 impairs cellular metabolism in aging adipose-derived stromal cells

Alice Nodari[1,*], Ilaria Scambi[1,*], Daniele Peroni[2,*], Elisa Calabria[1], Donatella Benati[1], Silvia Mannucci[1], Marcello Manfredi[3,4], Andrea Frontini[5], Silvia Visonà[6], Andrea Bozzato[7], Andrea Sbarbati[1], Federico Schena[1], Emilio Marengo[3,4], Mauro Krampera[8] and Mirco Galiè[1,‡]

ABSTRACT

Dysregulated immunity and widespread metabolic dysfunctions are the most relevant hallmarks of the passing of time over the course of adult life, and their combination at midlife is strongly related to increased vulnerability to diseases; however, the causal connection between them remains largely unclear. By combining multi-omics and functional analyses of adipose-derived stromal cells established from young (1 month) and midlife (12 months) mice, we show that an increase in expression of interferon regulatory factor 7 (IRF7) during adult life drives major metabolic changes, which include impaired mitochondrial function, altered amino acid biogenesis and reduced expression of genes involved in branched-chain amino acid (BCAA) degradation. Our results draw a new paradigm of aging as the 'sterile' activation of a cell-autonomous pathway of self-defense and identify a crucial mediator of this pathway, IRF7, as driver of metabolic dysfunction with age.

KEY WORDS: Aging, IFN signaling, Interferon regulatory factor 7, Cellular metabolism, Mitochondria, Branched-chain amino acid degradation

INTRODUCTION

Competition for food and response to infections are the major challenges for survival and evolution (Darwin, 1859; Fumagalli et al., 2011). To face these challenges, organisms have evolved complex strategies of metabolic adaptation and immunity. Their dysregulation (López-Otín et al., 2016; Franceschi et al., 2018b) is the major hallmark of the passing of time over the course of adult life and drastically increases vulnerability to diseases by midlife (midlife switch) (Berry et al., 2017; D'Antona et al., 2010; Manaye et al., 2013; Mori et al., 2012, 2014; Rogers et al., 2012; Schaum et al., 2020; Shoji et al., 2016; Timmons et al., 2019; Wu et al., 2014). Nevertheless, the mechanistic connection between metabolic and immune dysfunction with age is still largely unexplored. Some metabolic factors have been proposed that might sustain chronic inflammation with age (excess of nutrients, mitochondrial debris, misfolded and/or misplaced proteins), but very little is known about whether and how immune effectors might impact on metabolic homeostasis (Franceschi et al., 2018b).

Beside systemic immunity, all nucleated cells are endowed with a cell-autonomous, anciently conserved mechanism of self-defense to counteract microbial infection (MacMicking, 2012; Randow et al., 2013). This works as the first barrier against intruders and may eventually prime a systemic response. Type I interferons (IFN I) are the major effectors of cell-autonomous immunity (MacMicking, 2012). The nine members of the interferon regulatory factor (IRF) family of transcription factors (named IRF1 to IRF9) coordinate IFN I activation and function (Honda and Taniguchi, 2006). Along with IRF3, IRF7 is a master activator of IFN I (Honda et al., 2005) and interacts with other transcription factors (STATs, ATF-2, NFkB, CREB, AP-1) to modulate grading and diversification of IFN I-mediated responses (Levy et al., 2002; Wathelet et al., 1998). The IFN I network reprograms the expression of thousands of interferon-stimulated genes (ISGs) (Schneider et al., 2014; Schoggins et al., 2011), the impact of which on the biology of non-immune cells is largely unexplored (Levy et al., 2002; Wathelet et al., 1998).

We show herein that IRF7 expression increases with chronological age in adipose-derived stromal cells, driving impairment of mitochondrial function, amino acid biogenesis and branched-chain amino acid (BCAA) degradation. Our results identify IRF7 as major causal link between immune and metabolic dysfunctions that occur with age and draw a new paradigm of aging as the 'sterile' (i.e. in the absence of viral infection) activation of a cell-autonomous pathway of self-defense that impairs metabolic homeostasis and functions in a cell-autonomous fashion.

RESULTS

Age repatterns transcription of IFN-, mitochondrial- and amino acid-related genes and impairs mitochondrial function

Previous studies have shown that most age-related metabolic and neurodegenerative dysfunctions in rodents occur within the first half of life (up to 12 months of age) (Berry et al., 2017; D'Antona et al., 2010; Manaye et al., 2013; Mori et al., 2012, 2014; Rogers et al., 2012; Schaum et al., 2020; Shoji et al., 2016; Timmons et al., 2019). Adipose tissue is the central hub of metabolic (Rosen and Spiegelman, 2006) and immune regulation (Wu et al., 2007), and it represents an early sensor of the passing of time, as changes in its transcriptome precede those of other organs during adult life (Schaum et al., 2020). In a search for cell-intrinsic determinants of homeostatic alterations at middle age, we performed whole-genome transcriptional profiling of adipose-derived mesenchymal stromal

[1]Department of Neuroscience, Biomedicine and Movement, Section of Anatomy and Histology, University of Verona, 37134 Verona, Italy. [2]Department of Cellular, Computational and Integrative Biology, University of Trento, 38123 Trento, Italy. [3]Department of Sciences and Technological Innovation, University of Piemonte Orientale, 28100 Alessandria, Italy. [4]Center for Translational Research on Autoimmune and Allergic Disease – CAAD, University of Piemonte Orientale, 28100 Novara, Italy. [5]Department of Life and Environmental Sciences, Polytechnic University of Marche, 20121 Ancona, Italy. [6]Department of Public Health, Experimental and Forensic Medicine, University of Pavia, 27100 Pavia, Italy. [7]Department of Biomedical Sciences and Biotechnology, University of Brescia, 25123 Brescia, Italy. [8]Department of Medicine, Section of Hematology, Stem Cell Research Laboratory, University of Verona, 37134 Verona, Italy.
*These authors contributed equally to this work.

‡Author for correspondence (mirco.galie@univr.it)

A.B., 0000-0001-6409-1683; M.G., 0000-0002-6441-8313

Handling Editor: Daniel Billadeau
Received 26 October 2020; Accepted 26 April 2021

Journal of Cell Science (2021) 134, jcs256230. doi:10.1242/jcs.256230

cells (MSCs) explanted from 1-month-old (1mo; n=3) and 12-month-old (12mo; n=3) mice. To identify functional categories of genes that changed in a coordinated manner, we applied a gene set enrichment analysis (GSEA) approach (Subramanian et al., 2005) using a pre-compiled collection of genes belonging to Reactome functional annotation sets (Fabregat et al., 2016; Milacic et al., 2012; Vastrik et al., 2007) (Fig. 1A). In GSEA, genes in the dataset are first ranked based on their differential expression between the two experimental groups, and tests are then conducted on the ranked dataset to determine whether the gene sets of interest are randomly distributed or overrepresented among the genes upregulated in one group over the other. Cytokine and IFN signaling pathways were the most enriched functional categories in 12-month-old MSCs, while genes associated with respiratory electron transport had the highest enrichment scores (ES) in 1-month-old MSCs (Fig. 1B). GSEA using mitochondrial-related gene ontology (GO) terms (Ashburner

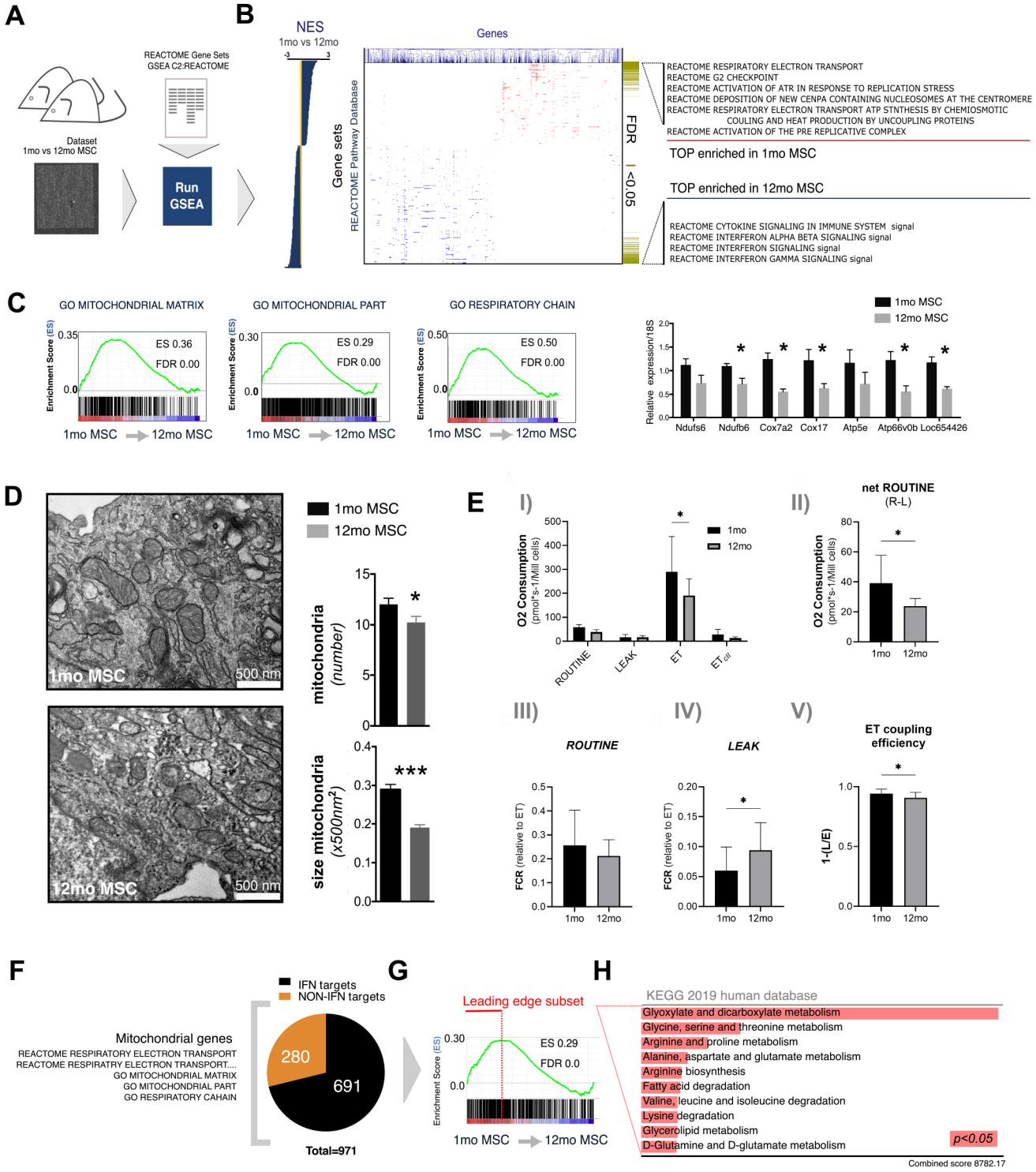

Fig. 1. See next page for legend.

Journal of Cell Science

Journal of Cell Science (2021) 134, jcs256230. doi:10.1242/jcs.256230

Fig. 1. Aging induces increased IFN signaling and diminished mitochondrial gene expression. (A) The microarray dataset of MSCs from 1-month-old (1mo) and 12-month-old (12mo) mice (n=3 per group) underwent GSEA with a pre-compiled collection of 480 gene sets from the Reactome functional category database. (B) Gene sets were ranked according to their normalized enrichment score (NES) (1-month-old MSCs versus 12-month-old MSCs), i.e. the ES normalized to the size of the sets. The most enriched gene sets in 1-month-old MSCs were related to mitochondrial genes and DNA repair mechanisms, while the most enriched in 12-month-old MSCs were related to the interferon signaling pathway. FDR, false discovery rate. (C) Left: GSEA using gene sets from the GO database confirmed the massive enrichment of different categories of mitochondrial genes in 1-month-old MSCs compared to 12-month-old MSCs. Plots show the ES profile across the ranked dataset. Right: qPCR analysis using more biological replicates (n=6 per group) confirmed the upregulation of selected mitochondrial genes in 1-month-old MSCs. Data are mean±s.e.m. expression relative to 18S rRNA. (D) Mitochondria were less abundant and were reduced in size in 12-month-old compared to 1-month-old MSCs. Electron micrographs shown are representative of three experiments. Data are mean±s.e.m. of 20 fields of view. (E) Mitochondrial function is impaired in 12-month-old MSCs in terms of uncoupled maximal oxidative capacity (ET) and net ROUTINE, expressed as rate of O_2 consumption (O_2 pmol/s per million cells; I and II), flux control ratios (FCRs; III and IV) and ET coupling efficiency (V). ET, maximal uncoupled oxidative capacity; ET_{cII}, maximal uncoupled oxidative capacity sustained by complex II following inhibition of complex I with rotenone; L, LEAK; R, ROUTINE. Data are the mean±s.d. of five experiments. (F) The mitochondria-related gene sets comprised 971 unique annotated transcripts. Amongst them, 691 were identified as ISGs, according to the INTERFEROME database. (G) These 691 genes were significantly enriched in 1-month-old versus 12-month-old MSCs. Leading edge analysis identified 221 genes that contributed the most to the ES. (H) The genes in the leading-edge subset were ontologically related to biochemical pathways of amino acid biosynthesis. *P<0.05; ***P<0.001 (unpaired t-test).

et al., 2000; The Gene Ontology Consortium, 2017) showed a significant enrichment of a large repertoire of mitochondrial genes encoding for structural and functional components, including mitochondrial matrix, ribonucleoproteins, aminoacyl-tRNA synthetases and regulators of mitochondrial biogenesis, in addition to components of the respiratory chain (Fig. 1C, left). Quantitative PCR (qPCR) analysis confirmed the overexpression of multiple oxidative phosphorylation (OXPHOS) genes in a larger cohort of freshly isolated MSCs (Fig. 1C, right). Consistent with increased mitochondrial gene expression, 1-month-old MSCs showed a higher number of mitochondria. In addition, the mitochondria of 1-month-old MSCs displayed a larger size and more structured cristae than those of 12-month-old MSCs (Fig. 1D). Analysis of mitochondrial respiration and function indicated quantitative and qualitative differences between 1-month-old and 12-month-old MSCs (Fig. 1E). Oxidative function was reduced overall in 12-month-old MSCs compared to that of 1-month-old MSCs (two-way ANOVA; P=0.03). Among the different respiratory states analyzed, oxygen consumption in the uncoupled maximal capacity of mitochondria (ET) state was 34% lower in 12-month-old MCSs compared to that in 1-month-old cells (P=0.01; Fig. 1E, panels I and II). Beside these quantitative data, qualitative analysis also revealed further differences in mitochondrial function between the two groups of MSCs. Indeed, data describing respiratory state expressed relative to the maximal ET capacity (flux control ratios, FCRs) indicated that, although no difference was found in the baseline unstimulated ROUTINE state (Fig. 1E, panel III), the fraction of oxygen consumption recorded in the unstimulated dissipative LEAK state in 12-month-old MSCs was higher compared to that of 1-month-old MSCs (56% higher; P=0.03; Fig. 1E, panel IV). Consistently, the net ROUTINE capacity (R-L), determined by physiological substrate uptake and cellular energy requirements, was higher in 1-month-old cells (69% higher; P=0.02). Furthermore, the ET coupling efficiency, accounting for matching between oxygen consumption and ATP production, was lower in the 12-month-old MSCs compared to that in the 1-month-old MSCs (4.2% lower; P=0.03; Fig. 1E, panel V). These results indicate that aging affects mitochondrial respiratory efficiency and leads to increased proton dissipation at the mitochondrial inner membrane.

The genes associated with the mitochondrial-related GO terms mentioned above (GO_MITOCHONDRIAL MATRIX, GO_MITOCHONDRIAL_PART, GO_RESPIRATORY-CHAIN; Fig. 1C, left) comprised 971 unique transcripts (Fig. 1F). Interestingly, among them, 691 (71%) were identified as IFN targets by the INTERFEROME database, a web-based repository of experimentally verified ISGs (Rusinova et al., 2013). This subset of mitochondrial genes was strongly enriched in 1-month-old MSCs relative to 12-month-old MSCs (Fig. 1G). Strikingly, the leading-edge subset – that is, the genes that contributed the most to the ES – comprised 221 genes mainly related to amino acid biosynthesis and BCAAs (Fig. 1H). This suggests that the age-induced changes in IFN signature might be the driving force of a multifaceted transcriptional reprogramming that impairs mitochondrial function and alters amino acid metabolism.

Age impairs amino acid metabolism

In line with our transcriptomic data, a comparison of the untargeted metabolomic profiles of 1-month-old and 12-month-old MSCs (Fig. 2) revealed a striking depletion of amino acids at middle age (Fig. 2A). Most of the key enzymes involved in amino acid biosynthesis were upregulated at the transcriptional level in 1-month-old MSCs compared with their expression in 12-month-old MSCs, especially those related to serine and glycine biosynthesis (Fig. 2B). The list of upregulated transcripts includes asparagine synthetase (*Asns*), an established readout of the activation of *Atf4*, which is the common transcriptional effector of downstream stress response pathways and the master regulator of amino acid biosynthesis-related genes (Harding et al., 2003).

Genes implicated in amino acid biosynthesis were identified as ISGs, according to the INTERFEROME database (Fig. S1A). Specifically, the promoters of these genes displayed motifs indicating regulation by various transcription factors activated by IFN type I and II regulators (Fig. S1B).

Having identified the transcriptional repression of genes implicated in amino acid biosynthesis, we also assessed the expression of genes implicated in amino acid degradation pathways. Most of the genes assessed had very low levels of expression, although they displayed a slight upregulation with age (Fig. 2C). In sharp contrast, branched-chain amino acid transaminase genes (*Bcat1* and *Bcat2*) displayed a higher expression and were downregulated with age. These *Bcat* genes encode two enzymes that catalyze the first step of the degradation of BCAAs (valine, leucine and isoleucine; Fig. 2D), yielding glutamate as a by-product. Hence, BCAT proteins are simultaneously implicated in amino acid degradation (of BCAAs) and synthesis (of glutamate). According to the INTERFEROME database, the transcriptional changes of the amino acid-related genes with age were consistent with the effects of IFN treatment (Fig. S1C).

To more robustly assess these transcriptional changes in amino acid metabolic pathways, we conducted a qPCR analysis of a greater number of biological replicates of differently aged MSCs (1-month-old MSC cells, n=8; 12-month-old MSC cells, n=6) (Fig. 2E). Although only *Bcat1* and *Psat1* showed changes in expression that reached statistical significance, we confirmed a coordinated downregulation with age of BCAA degradation-related and amino acid biosynthesis-related genes and the upregulation of amino acid degradation-related genes. However, we were not able to detect *Ido1* in our qPCR analysis.

Journal of Cell Science (2021) 134, jcs256230. doi:10.1242/jcs.256230

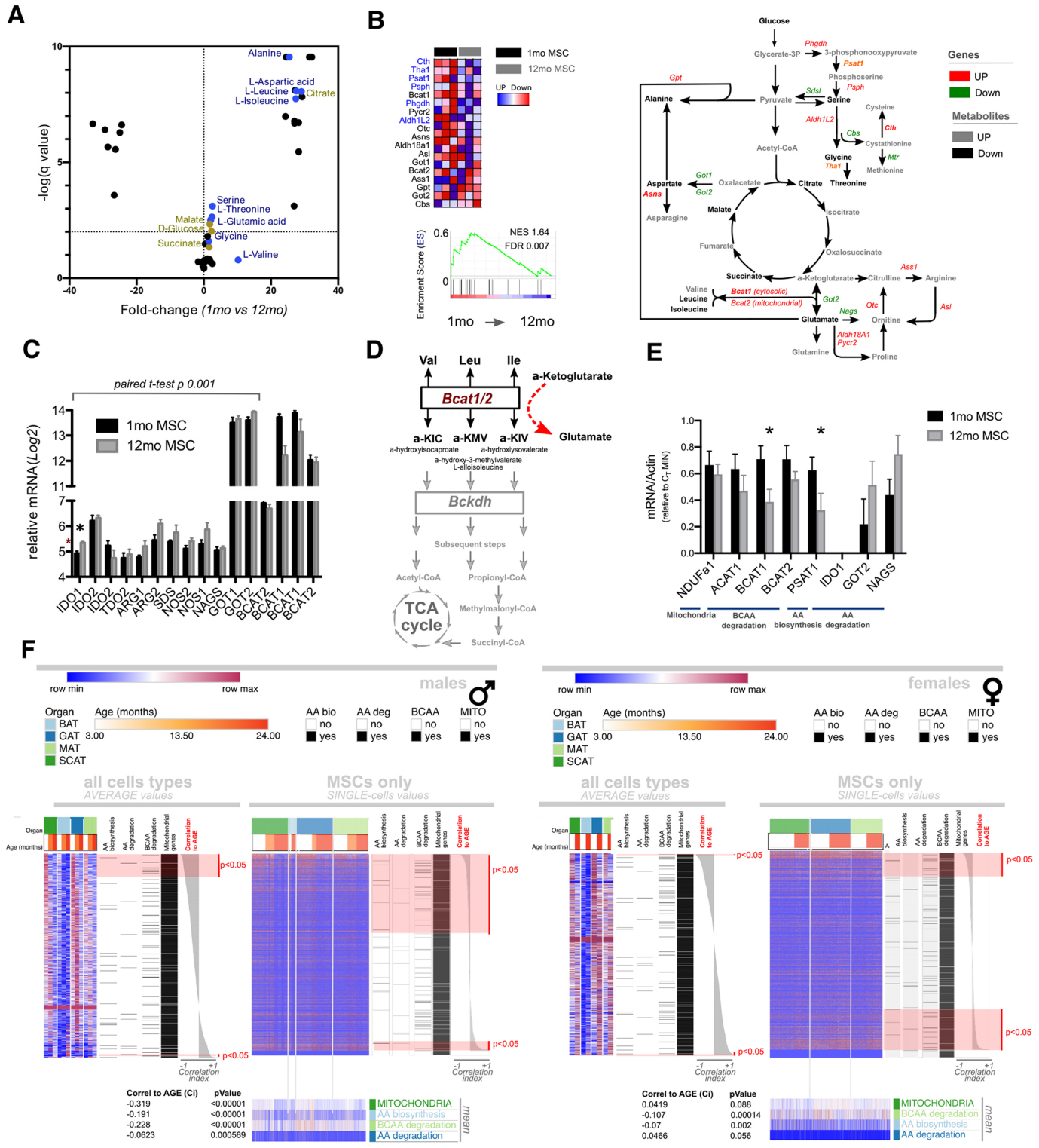

Fig. 2. See next page for legend.

In silico analyses confirm the downregulation of mitochondrial- and BCAA degradation-related genes with age

To further clarify these findings, we interrogated a recently published resource of single-cell transcriptomic data from 3-, 18- and 24-month-old mice (Consortium, 2020) (Fig. 2F). Specifically, we assessed the expression of genes related to mitochondria structure and function (the 971 genes indicated in Fig. 1F), amino acid biosynthesis (those listed in Fig. 2B), amino acid degradation (those listed in Fig. 2C) and BCAA degradation (those assigned to KEGG pathway mmu00280), in different deposits of adipose tissue (brown adipose tissue, BAT; gonadal adipose tissue, GAT; mesenteric adipose tissue, MAT; and subcutaneous adipose tissue, SCAT) either as an average of all cell types or as individual values of single resident MSCs, both in male

Journal of Cell Science (2021) 134, jcs256230. doi:10.1242/jcs.256230

Fig. 2. Aging suppresses amino acid biogenesis. (A) Gas chromatography–time of flight mass spectrometry (GC-TOF/MS) revealed many differences in the metabolomic profiles of 1-month-old (1mo) and 12-month-old (12mo) MSCs (n=3 per group). The list of metabolites that decreased with age included many amino acids. Fold change in metabolites is plotted against statistical significance [–log(q value)]. (B) GSEA showed a significant enrichment of genes encoding key enzymes of amino acid biosynthesis in 1-month-old versus 12-month-old MSCs (left panel), especially those involved in the serine and glycine biosynthesis (top left panel, blue). Most of these genes were either significantly (right panel, bold red) or non-significantly (right panel, red) upregulated in 1-month-old MSCs, while only 5 of 16 were (non-significantly) downregulated (right panel, green). FDR, false discovery rate; NES, normalized enrichment score. (C) Genes encoding the enzymes that catalyze amino acid degradation were slightly, but coordinately, upregulated in 12-month-old MSCs, with the exceptions of *Bcat1* and *Bcat2*. Microarray data expressed as mean±s.e.m. expression (n=3). (D) BCAT1 and BCAT2 catalyze the first reversible step of BCAA (Val, Leu and Ile) degradation. (E) qPCR analysis on a larger number of biological replicates (1mo MSC, n=8; 12mo MSC, n=6) confirmed the downregulation of the indicated representative mitochondria-, amino acid (AA) biosynthesis- and BCAA degradation-related genes and the concomitant upregulation of representative amino acid degradation-related genes. Data are mean±s.e.m. expression, normalized to actin. (F) Analogous changes in the transcriptional profile of mitochondria (MITO)-, amino acid biosynthesis (AA bio)- and BCAA degradation-related genes with age were confirmed in males by the analysis of a publicly available repository of single-cell transcriptomic data. Specifically, these gene sets were found to be significantly anti-correlated with age in all cell types (as average values, left-hand heatmaps) and single MSCs (right-hand heatmaps) from different deposits of adipose tissue of differently aged mice. *P<0.05 (unpaired t-tests in C and E).

and female animals. At least in males, we confirmed a strong anti-correlative relationship between age and expression of mitochondria-, BCAA degradation- and amino acid biosynthesis-related genes. Surprisingly, in sharp contrast with our model, amino acid degradation-related genes also displayed a negative correlation with age, although to a lesser extent. Of note, in line with data from our model, amino acid degradation-related genes were found to be expressed at very low level. Expression of *Ido1*, in particular, was undetectable. Taken together, these findings suggest that, although the effect of age on expression of amino acid degradation-related genes might be variable and context dependent, the downregulation of mitochondria-, amino acid biosynthesis- and BCAA degradation-related genes is inherently associated with aging in males.

IRF7 expression increases with age in multiple organs and tissues

In a search for molecular determinants underlying the transcriptional and metabolic dysregulation described above, we interrogated our microarray dataset (1-month-old versus 12-month-old MSCs, n=3 each) for the enrichment of gene sets comprising the targets of 615 different transcription factors (GSEA MSigDB collection c3.tft). The most highly enriched gene sets were related to the targets of the IRF family of transcription factors (Fig. 3A). Among the nine known members of the IRF family, the only ones readily upregulated in 12-month-old MSCs compared to their expression in 1-month-old MSCs were IRF7 and, to a lesser extent, IRF9 (Fig. 3B). This is in line with the STRING database (Szklarczyk et al., 2017), which reports IRF7 and IRF9 as displaying the highest frequency of co-expression among the IRFs (Fig. 3C). We confirmed a remarkable upregulation of IRF7 mRNA and protein (Fig. 3D) in 12-month-old MSCs compared to the expression in 1-month-old MSCs. Previously identified IRF7-specific targets (Puthia et al., 2016) were also significantly enriched in older MSCs (Fig. 3E).

The increase of IRF7 expression with age was not restricted to MSCs, since we found IRF7 protein to be upregulated in skeletal muscle (both gastrocnemius and quadriceps), adipose tissue and lungs (but not the spinal cord) of 8-month-old mice (n=3) compared to 1-month-old mice (n=3) (Fig. 3F, upper panels). qPCR analysis confirmed the downregulation of mitochondria-, amino acid biosynthesis- and BCAA degradation-related genes in 8-month-old adipose tissue and lung, whereas amino acid degradation-related genes, such as *Got1* and *Ido1*, were upregulated or unchanged (Fig. 3F, lower panels).

To further support our findings, we assessed how the transcriptional change of *Irf7* with age might correlate with expression of metabolic genes using a recently published dataset that comprises RNA-seq profiling of multiple organs (gastrocnemius, kidney, liver and hippocampus) from differently aged (6, 9, 12, 18, 21, 24 and 27 months) rats (Shavlakadze et al., 2019) (Fig. 3G). Once again, the analysis confirmed the upregulation of IRF7 expression with age, and its inverse correlation with expression of mitochondria- and BCAA-related genes in different organs (gastrocnemius, kidney and liver, but not hippocampus), whereas how age correlates with expression of amino acid biosynthesis- and degradation-associated genes remains more controversial.

In addition, we surveyed the expression of *Irf7* transcripts across additional publicly available datasets from the Gene Expression Ominibus (GEO) database (Fig. S2) and confirmed upregulation of *Irf7* expression at either middle or old age in most tissues and organs (skeletal muscle, adipocytes, heart, kidney, brain and lung) across multiple species. We then interrogated the same GEO datasets for the enrichment of gene sets related to mitochondrial biogenesis and function, translation and amino acid metabolism (Fig. 3H). In line with the data from MSCs, younger samples across the GEO datasets displayed a strong enrichment of genes related to mitochondrial components, mitochondrial translation machinery and, to a lesser extent, aminoacyl-tRNA biosynthesis. Conversely, older samples displayed an enrichment of genes related to amino acid deprivation. Collectively, these data suggest that IRF7 expression increases with age in multiple tissues across different species and correlates with the downregulation of mitochondria- and BCAA degradation-related genes.

IRF7 knockdown reverts IFN signaling and restores mitochondrial biogenesis

The above data points to IRF7 as the causal connection between increased interferon signaling and dysregulated cellular metabolism over adult life. To definitively test this hypothesis, we knocked-down IRF7 in 12-month-old MSCs (shIRF7; Fig. 4A) and executed a new whole-genome microarray profiling. Genes that had significantly (t-test; P<0.05) downregulated expression in shIRF7 MSCs were enriched in functional categories related to the antiviral immune response, thus clearly validating the loss of IRF7 function (Fig. 4B; Fig. S3). On the other hand, genes significantly upregulated in 12-month-old shIRF7 MSCs were predominantly enriched in mitochondrial- and electron transport-related genes (Fig. 4B; Fig. S3). To identify the functional categories of genes that were altered in aging and reversed by IRF7 knockdown, we performed GSEA with the Reactome collection of gene sets and plotted the ES values of 12-month-old control (Ctrl) MSCs versus shIRF7 MSCs against the respective ES value of 1-month-old versus 12-month-old MSCs. Strikingly, interferon signaling pathway- and oxidative phosphorylation-related gene sets hit the top up and top down positions, respectively (Fig. 4C). In addition, genes related to ‘mitochondrial-matrix’, ‘respiratory chain’ and ‘mitochondrial-part’ GO categories were significantly enriched in 12-month-old shIRF7 cells compared to 12-month-old control cells (Fig. 4D). In accordance

Journal of Cell Science (2021) 134, jcs256230. doi:10.1242/jcs.256230

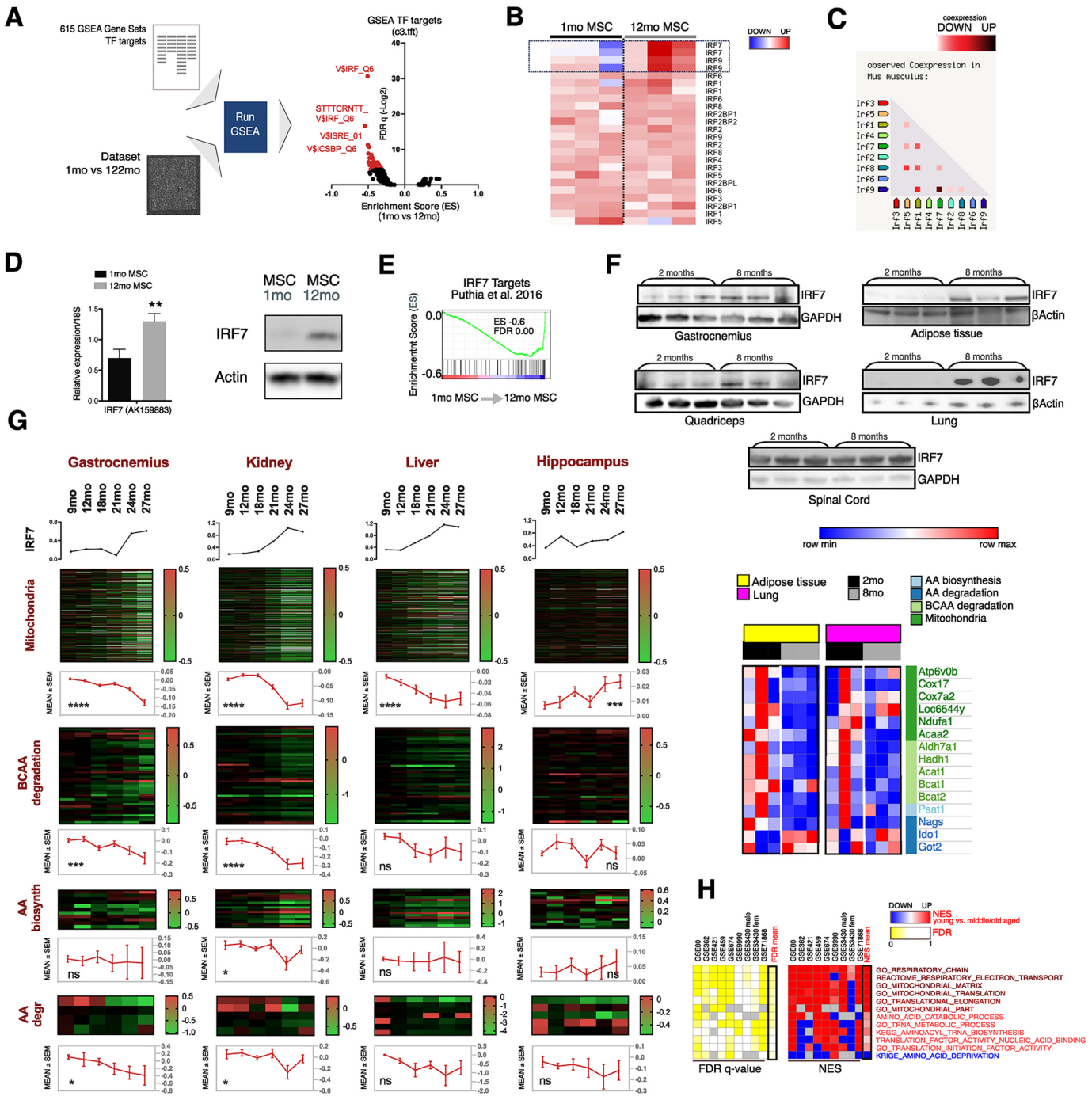

Fig. 3. See next page for legend.

with the transcriptional data, 12-month-old shIRF7 cells showed a significantly greater number of mitochondria displaying more structured cristae compared to controls (Fig. 4E).

IRF7 knockdown restores mitochondrial function

To determine whether, besides affecting the expression of mitochondrial gene sets and mitochondrial morphology, IRF7 depletion is also relevant for mitochondrial function, we compared, using high-resolution respirometry (HRR), the rates of oxygen consumption of intact 12-month-old shIRF7 cells and 12-month-old control cells, in which metabolic responses are essentially based on endogenous substrates (Fig. 5A–C). A coupling control protocol was used to investigate the different respiratory states (ROUTINE, LEAK and ET). The ET state induced by stepwise titration of the uncoupler (CCCP) was significantly increased by 25% (P=0.02) in 12-month-old shIRF7 cells compared to that in controls (Fig. 5A). Data normalized relative to the ET (FCRs) showed that 12-month-old shIRF7 cells had reduced oxygen consumption in the basal ROUTINE (P=0.004) state as well in the dissipative LEAK state (~50% reduction; P=0.02) (Fig. 5B). Lower oxygen consumption by 12-month-old shIRF7 cells in the ROUTINE and LEAK states was accompanied by an increase of the ET coupling efficiency, expressed as 1−(LEAK/ET) (32% increase; P=0.038; Fig. 5C). These results indicate that IRF7 knockdown improves

Journal of Cell Science (2021) 134, jcs256230. doi:10.1242/jcs.256230

Fig. 3. IRF7 expression increases with aging. (A) Using the GSEA algorithm, we interrogated the transcriptomic profiles of 1-month-old (1mo; *n*=3) and 12-month-old MSC (12mo; *n*=3) samples for the enrichment of a precompiled collection of 615 gene sets of transcription factor motifs based on the work of Xie et al. (2005) (GSEA TF targets c3.tft). Genes upregulated in 12-month-old versus 1-month-old MSCs were enriched in motifs related to the interferon regulatory factor (IRF) family of transcription factors. (B) Among the nine members of this family, IRF7 and, to a much lesser extent, IRF9 (dashed box) were the only ones whose transcripts were readily upregulated in 12-month-old compared to 1-month-old MSCs. (C) STRING analysis revealed that IRF7 and IRF9 are frequently co-regulated. (D) 12-month-old MSCs exhibited increased levels of IRF7 expression with respect to both transcript (left) and protein (right) abundance. Data are mean±s.e.m. of three experiments. Blots are representative of three experiments. Actin is shown as a loading control. (E) IRF7 expression levels, as shown in D, are consistent with a significantly elevated level of the transcriptional expression of genes previously identified as IRF7 targets, as shown by enrichment analysis (FDR, false discovery rate). (F) Top: IRF7 protein levels were elevated in multiple organs (gastrocnemius, quadriceps, adipose tissue and lungs), but not in spinal cord, of 8-month-old mice (*n*=3) compared to 2 month-old mice (*n*=3). GAPDH is shown as a loading control. Bottom: IRF7 increase with age in adipose tissue and lung samples was concomitant with diminished expression of representative mitochondria-, amino acid (AA) biosynthesis- and BCAA degradation-related genes, while amino acid degradation-related genes were upregulated (adipose tissue) or unchanged (lungs). (G) The analysis of a recently published RNA-seq data resource (Shavlakadze et al., 2019) comparing various organs of differently aged rats reveals that the upregulation of IRF7 expression with age is closely correlated with diminished expression of mitochondria-, amino acid biosynthesis- and BCAA degradation-related genes in gastrocnemius, kidney and liver, but not in hippocampus. (H) GSEA analysis of publicly available datasets from the GEO database reveals the reduced expression of mitochondrial- and translation-related genes and increased expression of amino acid deprivation-related genes with age in multiple organs and tissues of multiple species. NES, normalized enrichment score. **P*<0.05; ***P*<0.01; ****P*<0.001; *****P*<0.0001; ns, not significant (D, unpaired *t*-test; G, ANOVA test for linear trend).

mitochondrial respiratory efficiency, probably due to a greater integrity of mitochondrial inner membranes and, thus, a reduced proton leak.

IRF7-induced improvement of OXPHOS function is linked to complex I

To dissect the impact of IRF7 knockdown on mitochondrial fitness in greater depth, we permeabilized 12-month-old shIRF7 and control cells to allow the entry of specific substrates and compared their mitochondrial respiration using HRR assays in the ROUTINE, LEAK, OXPHOS and ET respiratory states. To investigate the effects of IRF7 depletion on fatty acid- and NADH-dependent pathways we sequentially added octanoylcarnitine fatty acid (FA) and malate (ETF-linked); malate and glutamate (complex I-linked); and succinate substrates (complex II-linked). These conditions, following ADP stimulation, allow determination of the relative contribution to OXPHOS of β-oxidation, complex-I and complex-II, respectively. Qualitative analysis of FCRs allowed us to evaluate the relative contribution of the various complexes to mitochondrial respiration and highlighted significative qualitative differences between 12-month-old shIRF7 cells and control cells. Fatty acid-dependent pathways in the OXPHOS state (P_{OM}) were activated at significantly lower levels in 12-month-old shIRF7 cells compared to activation in 12-month-old control cells (19% lower; *P*=0.02; Fig. 5D). In addition, investigating the effect of addition of glutamate (G) in the OXPHOS respiratory state, using the control factor $P_{OMG}-(P_{OM}/P_{OMG})$, we observed a remarkable stimulation in 12-month-old shIRF7 cells compared to 12-month-old ctrl cells (80% increase; *P*=0.02; Fig. 5E), suggesting that IRF7 knockdown renders mitochondria more responsive to glutamate stimulation.

IRF7 knockdown partially restores the amino acid pool and increases BCAA degradation

The amino acids depleted in 12-month-old cells were all partially restored upon IRF7 knockdown, with the exception of the BCAAs leucine and isoleucine (Fig. 6A). However, we did not find coordinated changes in the transcription of genes involved in either amino acid biosynthesis or degradation (Fig. 6B). This drives us to speculate that the rescue of the amino acid pool after IRF7 knockdown relies on alternative pathways. The fact that, unlike other amino acids, leucine and isoleucine were not restored suggests that IRF7 knockdown allows the BCAA degradation pathway to feed into the TCA cycle (anaplerosis) to sustain an accelerated flux of intermediates (oxalacetate) for amino acid biosynthesis (Fig. 6C). In line with this model, genes involved in BCAA degradation were drastically enriched in 12-month-old shIRF7 cells compared to control cells (Fig. 6D). Remarkably, we found a significant upregulation of the gene encoding PP2Cm (*Ppm1K*), the mitochondrially localized enzyme that activates the branched-chain α-keto acid dehydrogenase (BCKDH) complex, which is the rate-limiting enzyme of the BCAA degradation pathway, and loss of which has been reported to impair mitochondrial function, increase oxidative stress, and promote abnormal cardiac and neural development (Lu et al., 2007, 2009). We also found increased transcript levels of krueppel-like factor 15 (*Klf15*) (Fig. 6D), which has been previously shown to be a master inducer of BCAA degradation genes and crucial for prevention of mitochondrial dysfunction and oxidative stress in heart (Gray et al., 2007; Sun et al., 2016a,b). Also, IRF7 knockdown completely cleared the age-induced methylmaleic acid (citraconic acid), which is a by-product and established diagnostic biomarker of deranged isoleucine degradation (Duran et al., 1978) (Fig. 6E). BCAA degradation may feed the TCA cycle by providing succinyl-CoA, which is converted to succinate by succinate CoA-ligase GDP-forming beta subunit (*SuclG2*). Accordingly, succinate was more abundant in 12-month-old shIRF7 cells compared to levels in control cells, and *SuclG2* expression was significantly upregulated (*P*=0.03; Fig. 6E). Oxalacetate did not accumulate in 12-month-old shIRF7 cells compared with levels in control cells, despite expression of the enzyme that generates it from malate, malate dehydrogenase 1 (encoded by *Mdh1*), being markedly upregulated (*P*=0.07) and expression of the enzyme that converts oxalacetate to citrate (citrate synthase, encoded by *Cs*) being downregulated in the 12-month-old shIRF7 cells (Fig. 6E). This suggests that the rate of oxalacetate generation equals the rate of its cataplerotic diversion toward extra-TCA cycle pathways. Accordingly, expression of the cytoplasmic and mitochondrial isoforms of the enzyme that converts oxalacetate to aspartate (glutamic oxalacetic transaminase-1 and -2, encoded by *Got1* and *Got2*, respectively) were slightly but coordinately upregulated in shIRF7 cells. Finally, the vast majority of the enzymes involved in the TCA cycle were upregulated in 12-month-old shIRF7 cells (paired *t*-test; *P*=0.06), which supports an increased TCA cycle rate (Fig. 6C).

Confirming that IRF7 knockdown can drive the increase in TCA cycle rate, INTERFEROME analysis revealed that all the TCA cycle genes that were upregulated in 12-month-old shIRF7 cells are ISGs and, as such, might be regulated upon IFN treatment (Fig. S4A,B). The same applied for genes involved in BCAA degradation (Fig. S4C,D).

IRF7 impairs 'core' longevity pathways

Collectively, our data indicate that aging induces the sterile activation of IRF7-mediated metabolic programming, impairing

Journal of Cell Science (2021) 134, jcs256230. doi:10.1242/jcs.256230

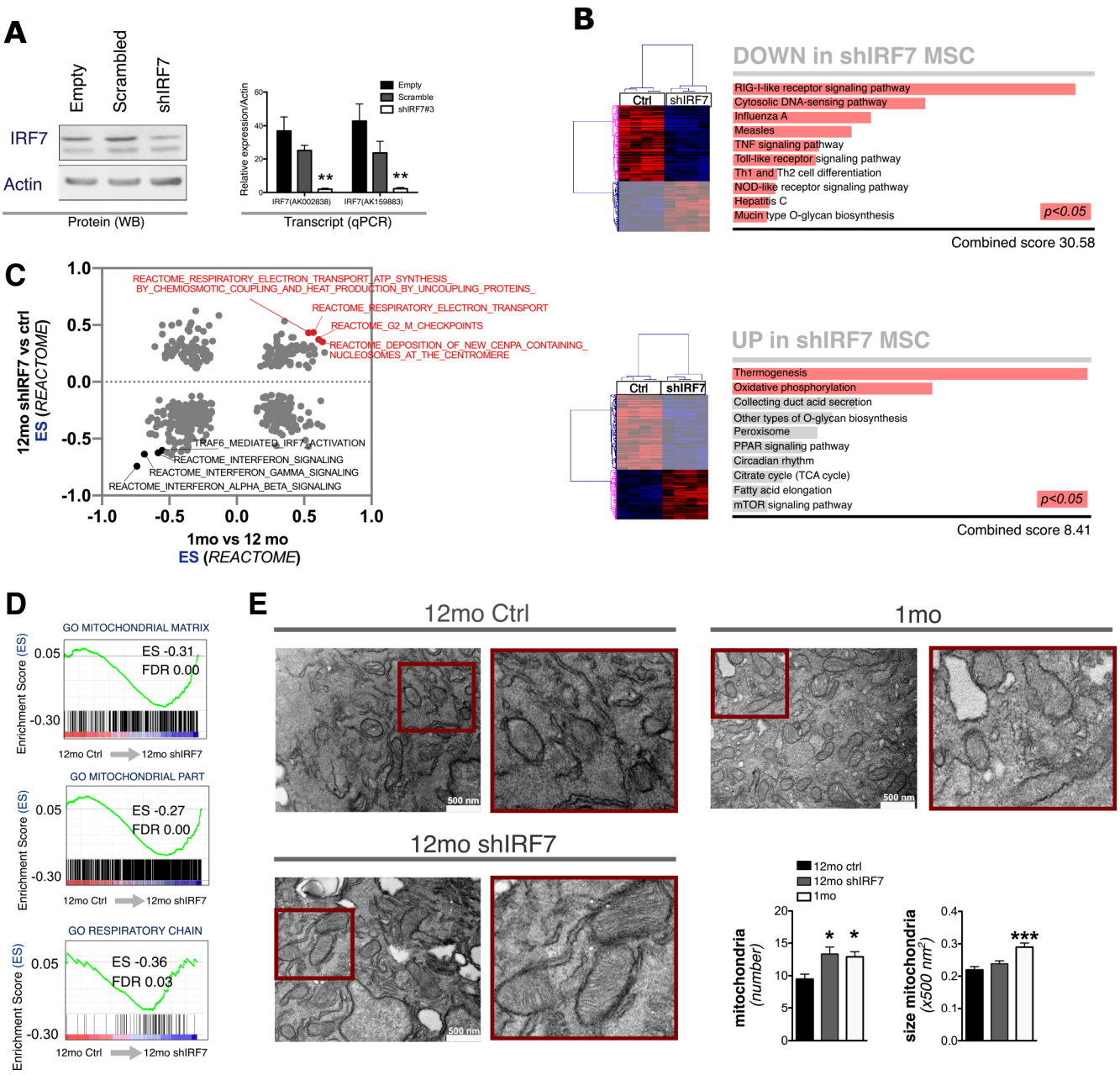

Fig. 4. IRF7 silencing reverts mitochondrial gene expression and function. (A) IRF7 was knocked down in 12-month-old (12mo) MSCs using shRNA (shIRF7). Knockdown of IRF7 expression was assessed by western blotting (WB) and qPCR, as compared to expression in cells transformed with empty vector or control scrambled shRNA. Blot is representative of three experiments, with actin shown as a loading control. qPCR data are mean±s.e.m. of three experiments. Transcriptional changes in shIRF7 MSCs were subsequently assessed though a whole-genome microarray analysis (n=4 per group). (B) Genes with significantly different expression (t-test, P<0.05) in 12-month-old shIRF7 versus 12-month-old control (Ctrl) MSCs were functionally categorized based on the KEGG 2019 mouse algorithm. In the heatmaps, red indicates increased expression and blue indicates decreased expression. (C) ES values of the Reactome gene sets for the '12-month-old control versus 12-month-old shIRF7 MSC' microarray dataset were calculated using GSEA and plotted versus the corresponding ES values for the '1-month-old versus 12-month-old MSC' dataset. (D) GSEA analysis for three distinct mitochondria-related gene sets from the Gene Ontology Consortium Database confirmed the enrichment of mitochondrial genes in 12-month-old shIRF7 MSCs compared to controls. (E) Mitochondria in shIRF7 MSCs were significantly more abundant and displayed more structured cristae than those of control MSCs. Boxes indicate regions shown in magnified images on the right. Micrographs are representative of three experiments. Data are mean±s.e.m. of 20 fields of view. *P<0.05; **P<0.01; ***P<0.0001 (A, t-test; E, one-way ANOVA with Dunnett post-hoc test compared to 12-month-old controls).

mitochondrial and amino acid biogenesis (Fig. S5). Since viruses rely on the bioenergetic and biosynthetic machinery of the host for their replication (Walsh and Mohr, 2011), it can be postulated that IFN signaling counteracts viral spread by shutting down 'core' metabolic pathways of the host and that an overwhelming response may lead to severe impairment of cell and organ functions.

DISCUSSION

The detrimental effects of aging manifest early in the course of adult life (Berry et al., 2017; D'Antona et al., 2010; López-Otín et al., 2013; Mori et al., 2012, 2014; Rogers et al., 2012; Shoji et al., 2016; Timmons et al., 2019). The molecular determinants of aging have recently been proposed to follow a non-linear progression rate,

Journal of Cell Science

Journal of Cell Science (2021) 134, jcs256230. doi:10.1242/jcs.256230

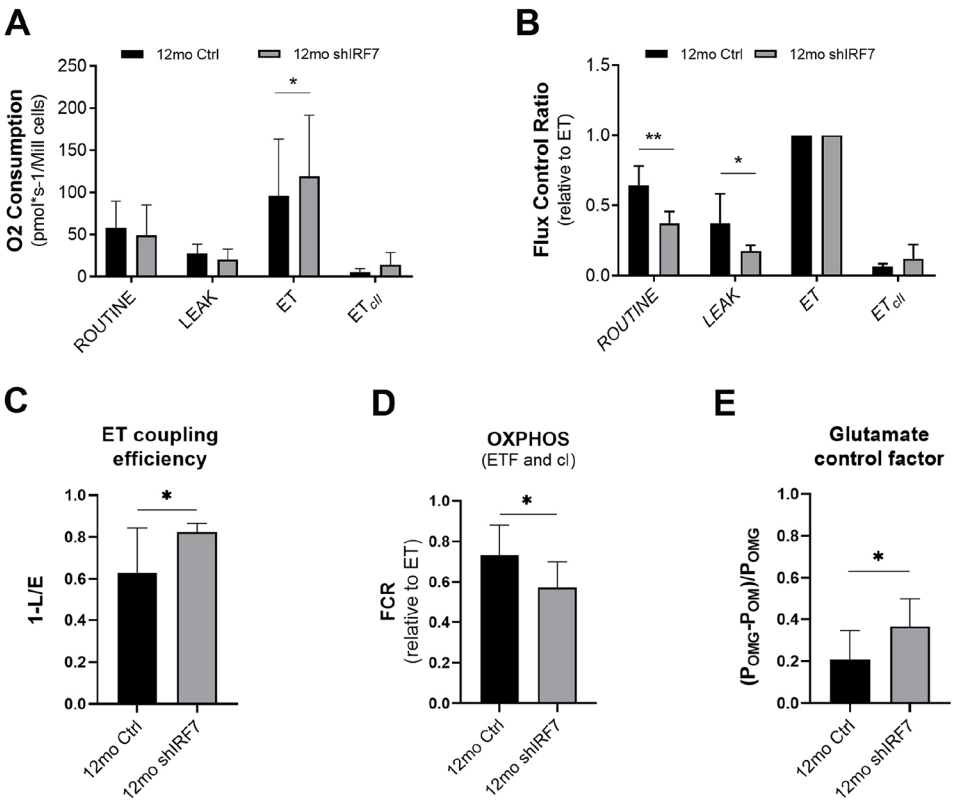

Fig. 5. Mitochondrial function evaluated using high-resolution respirometry in 12-month-old control and shIRF7 cells. (A) Quantitative analysis of the rate of oxygen consumption (expressed as O_2 pmol/s per million cells) in the ROUTINE, LEAK and ET respiratory states (ET_{cII}, ET sustained by complex II following inhibiton of complex I with rotenone) in intact 12-month-old control (12mo Ctrl, black) or 12-month-old shIRF7 (12mo IRF7, gray) cells. (B) Qualitative analysis of data of mitochondrial function in intact cells expressed relative to ET (flux control ratio, FCR) in the respiratory states analyzed (ROUTINE, LEAK and ET). (C) ET coupling efficiency was expressed as 1−(L/E). (D) FCRs in the ADP-stimulated OXPHOS state sustained by ETF and complex I (P_{OM}) in 12-month-old control or 12-month-old shIRF7 permeabilized cells. (E) Effect of addition of glutamate in 12-month-old control and 12-month-old shIRF7 permeabilized cells evaluated using the control factor $(P_{OMG}-P_{OM})/P_{OMG}$. Data are reported as mean±s.d., n=5. *P<0.05; **P<0.01 (two-way ANOVA with Sidak's post-hoc correction in A,B; paired t-test in C–E).

with a boost at middle age (midlife switch) (Timmons et al., 2019) that drastically impairs body fitness and increases vulnerability to metabolic, cardiovascular, locomotory and neurodegenerative disorders, among many others. As such, according to the 'geroscience hypothesis', the discovery of novel therapeutic strategies capable of preventing the general process of aging is a more straightforward challenge than fighting each specific age-related disorder individually (Franceschi et al., 2018a).

We show herein that the increased expression of IRF7 during aging leads to the sterile activation of cell-autonomous pathways of self-defense, which impairs crucial metabolic functions, such as mitochondrial and amino acid biogenesis and BCAA degradation. Our results contribute to draw a novel paradigm in cell biology, setting a causal link between cell-autonomous pathways of self-defense and mitochondrial-centered metabolic pathways, such as respiration, amino acid biosynthesis and BCAA degradation.

IFNs regulate the transcription of thousands of genes (ISGs) (MacMicking, 2012; Randow et al., 2013). Although the anti-viral effect of some of these genes is partially clear, the effect of their global repatterning on host cell biology is virtually unexplored. Nevertheless, the IFN-mediated response must be finely tuned, as its dysregulated activation may become detrimental (Baruch et al., 2014; Channappanavar et al., 2016; Davidson et al., 2014; Major et al., 2020; Teijaro et al., 2013). Our results drive us to speculate that one of the major aims of the IFN-mediated response is to shut down the bioenergetic and biosynthetic machinery of the host, which would be otherwise usurped by the virus for its own replication (Walsh and Mohr, 2011). The cost:benefit ratio for the host is never obvious, but the opportunity for the cell to embark on such a potentially harmful program might be justified when a real microbial attack occurs. What is less clear is why and how age might activate this program in the absence of viral infection.

Nevertheless, a generalized shutdown of crucial metabolic functions may help to explain many aspects of the pathophysiology of aging-related disorders. Mitochondrial and amino acid biogenesis are common outcomes of the ancient evolutionarily conserved programs referred to as the integrated stress response (ISR) (Harding et al., 2003; Pakos-Zebrucka et al., 2016). These pathways act constitutively as quality control mechanisms and are massively invoked to face multiple acute or chronic stress conditions, such as nutrient deprivation, an oxidative environment, proteotoxic stress and overloading of the endoplasmic reticulum (Harding et al., 2003; Quirós et al., 2017). The moderate stimulation of these pathways is the basis of the beneficial effects of mild stress interventions, such as dietary restriction, in preventing aging and even prolonging life span (Zid et al., 2009; Mazière et al., 1999). Mitochondria are both targets and master regulators of these stress response programs. Beyond their bioenergetic role, mitochondria have evolved as signaling organelles that instruct nuclear transcription, cytosolic protein translation and metabolic rewiring to coordinate cellular adaptation to environmental changes (Cardamone et al., 2018; Chandel, 2015; Quirós et al., 2017; Suhm et al., 2018; Wrobel et al., 2015). Hence, maintenance of proper mitochondrial activity is a priority challenge for cells and organs, and one that should be accomplished in favor of stress-induced adaptive rearrangements (Harding et al., 2003; Pakos-Zebrucka et al., 2016). The observation that mitochondria of 12-month-old shIRF7 cells showed a reduced OXPHOS capacity sustained by fatty acids suggests that these cells may accumulate lower levels of reactive oxidant species (ROS), which are generally accumulated during β-oxidation (Mazière et al., 1999). This condition could explain the improved quality of mitochondrial membranes, consistent both with the enhanced coupling efficiency and improved morphology of the mitochondrial membranes. We cannot say at this stage whether the increase in mitochondrial number and function might be the direct effect of IRF7 knockdown or just a consequence of a chain of events

Journal of Cell Science (2021) 134, jcs256230. doi:10.1242/jcs.256230

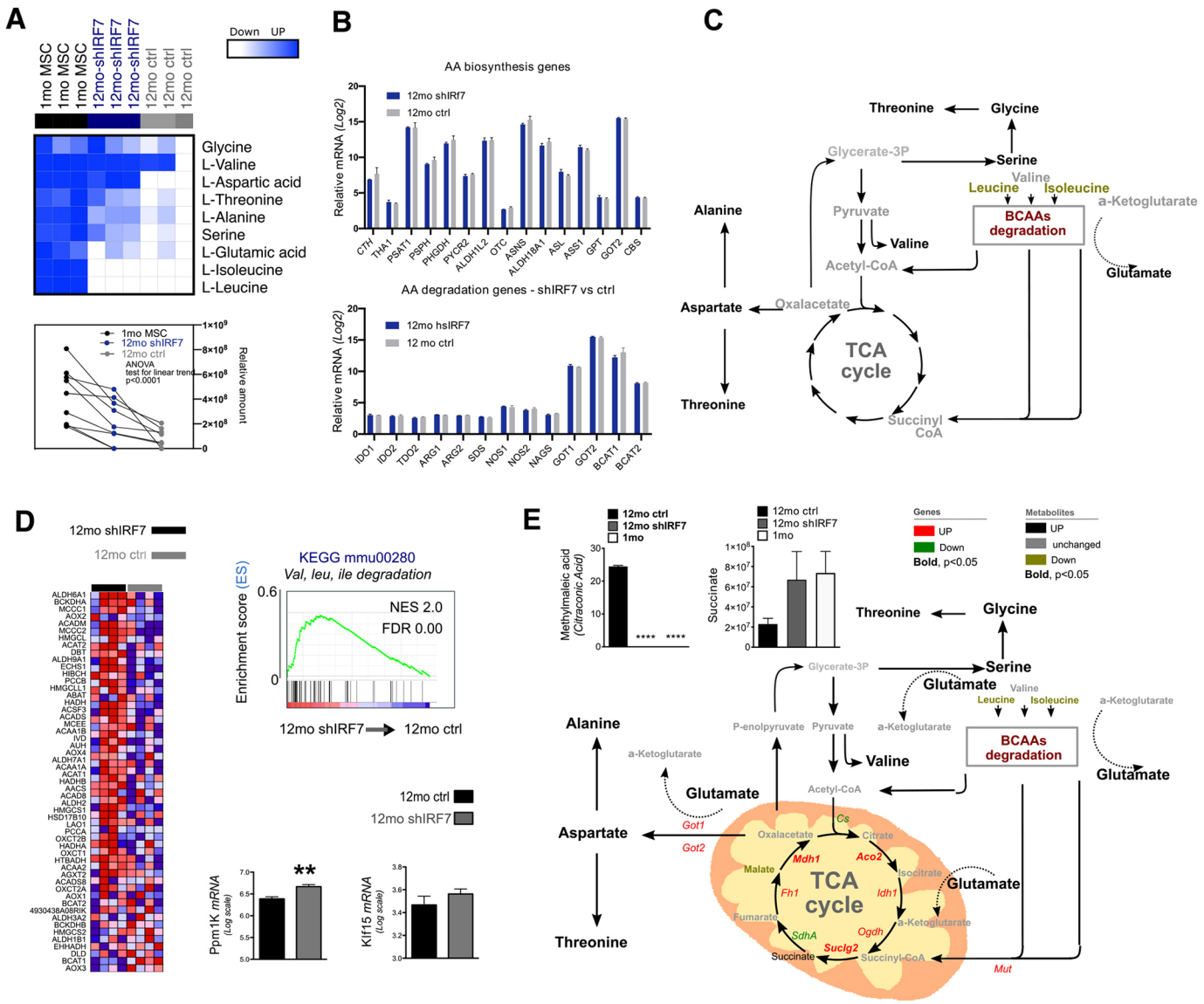

Fig. 6. IRF7 knockdown partially restores the intracellular amino acid pool. (A) Metabolomic analysis reveals that all amino acids reduced in middle-aged (12-month-old; 12mo ctrl) cells are restored upon IRF7 knockdown (12mo-shIRF7), except leucine and isoleucine. Graph (bottom) shows the average amount of these amino acids in 1mo MSC, 12mo shIRF7 and 12mo ctrl cells. (B) Expression of genes encoding enzymes involved in either amino acid (AA) biosynthesis or degradation is not coordinately changed upon IRF7 knockdown. Data are mean±s.e.m. of three experiments. (C) BCAA degradation provides glutamate and feeds into the TCA cycle, serving as a common precursor of aspartate, alanine, serine and glycine. (D) Genes encoding enzymes involved in BCAA-degradation pathways and their major regulators (such as *Ppm1k* and *Klf15*) are enriched upon IRF7 knockdown. Heatmap (left) shows the expression of KEGG mmu00280 genes (red, upregulated; blue, downregulated). Top right: GSEA (FDR, false discovery rate; NES, normalized ES). Bottom right: quantification of *Ppm1k* and *Klf15* expression in the microarray dataset. (E) Genes encoding enzymes that catalyze the various steps of the TCA cycle are significantly upregulated (red, bold), non-significantly upregulated (red) or non-significantly downregulated (green) upon IRF7 knockdown. Graphs show the levels of methylmaleic acid and succinate in 12-month-old control and shIRF7, and 1-month-old control cells. Data are mean±s.e.m. of microarray data. The metabolomic and transcriptional profiles suggest a model in which BCAA degradation feeds the TCA cycle to sustain amino acid biogenesis. $^{**}P<0.01$; $^{****}P<0.0001$ (unpaired *t*-test).

that result in a youthful phenotype. What is clear is that changes in IRF7 and IFN signaling with age might impact on cellular metabolism that involves mitochondria-centered pathways such as cellular respiration, amino acid biosynthesis and BCAA degradation.

BCAA degradation has been extensively implicated in aging and aging-related diseases. Specifically, an increased amount of circulating BCAAs and related metabolites is strongly associated with obesity, type 2 diabetes and heart disease (Felig et al., 1969; Newgard et al., 2009; Huffman et al., 2009; Li et al., 2017; Lynch and Adams, 2014; Turer et al., 2009). Conversely, increased expression of genes related to BCAA degradation correlates with insulin sensitivity and boosts fatty acid oxidation (Lerin et al., 2016; Papathanassiu et al., 2017). BCAA supplementation supports cardiac and skeletal muscle mitochondrial biogenesis, prevents oxidative damage and promotes exercise capacity in middle-aged animals (D'Antona et al., 2010).

Previous studies have explored the reciprocal causal connections between mitochondria and inflammation, and their possible role in aging. Recent studies have shown that mitochondrial disruption may trigger inflammatory reactions (Garaude et al., 2016; Jin et al., 2014; Zhang et al., 2010), whereas pro-inflammatory mediators may contribute, in turn, to alteration of mitochondrial activity

Journal of Cell Science (2021) 134, jcs256230. doi:10.1242/jcs.256230

(López-Armada et al., 2006). However, mechanisms modeled in these studies implicate the systemic recruitment of immune cells (neutrophils and macrophages) (Franceschi et al., 2017; Jin et al., 2014), circulating pro-inflammatory cytokines (TNF, IL6 and IL1) (López-Armada et al., 2006; van Horssen et al., 2017), cell debris (Zhang et al., 2010) or DNA-damaging chemical mediators (such as reactive oxygen species and reactive nitrogen species) (Garaude et al., 2016; Kim et al., 2010) and have ultimately contributed to establishing the prevailing notion that aging-related deterioration of tissue function and mitochondrial integrity relies on a complex bi-directional interaction between systemic immunity and tissue-resident cells. We provide herein an additional, cell-intrinsic perspective that envisions the age-related mitochondrial dysfunction of non-immune cells as the consequence of 'cell-autonomous' alterations of immunity-related signaling pathways. IRF7 functions as the molecular trigger of these pathways during aging. Whether the increased expression of IRF7 with age is primed by extrinsic or intrinsic factors is not clear. Nevertheless, its impact on the transcription of immune and mitochondrial genes is cell autonomous (as it persists in cultured cells over multiple passages) and reversible, thus ruling out the involvement of the genetic damage eventually induced by ROS and NOS, which has previously been implicated in connecting inflammatory responses with mitochondrial integrity. The role of IRF7 as a regulator of immune cell function has been extensively investigated by thousands of studies. In sharp contrast, its expression and function in non-immune cells remains unexplored. Our data demonstrate that the role of IRF7 extends beyond the protection against external intruders and that its gain of function may indeed represent an intrinsic paradigm for the degeneration that occurs during adulthood. Our results suggest that IRF7 is an ideal target for the development of therapies that are potentially effective against multiple and intersecting aspects of the aging phenotype.

MATERIALS AND METHODS

Isolation of adipose-derived MSCs

The inguinal fat pads of FVB male mice aged 1 (n=8) and 12 (n=8) months were surgically excised, weighed and processed to isolate the adipose-derived stromal cells, according to standard protocols (Peroni et al., 2008). Briefly, the extracellular matrix was digested with collagenase (1 mg/ml) and centrifuged to obtain a high-density pellet, the stromal vascular fraction (SVF). After centrifugation, the SVF cell number was determined using light microscopy, and the cells were plated at a concentration of 10^5 cells/cm^2 in DMEM medium (GIBCO) with high glucose concentration (GLUTAMAX I, GIBCO; 10% FCS, GIBCO; 100 U/ml penicillin; and 100 µg/ml streptomycin). After 2–3 weeks of culture, a homogeneous cell population was obtained. The cells were identified as MSCs on the basis of their immunophenotype. Specifically, the positivity of CD106 (VCAM1), CD73 (NT5E), CD29 (ITGB1), CD44, CD90 (THY1) and the lack of hematopoietic (as detected using CD45, CD14, CD11c, CD123 and CD34 monoclonal antibodies) and endothelial cell markers (as detected using CD31 monoclonal antibody) were assessed by means of cytofluorimetric analysis. Animals were handled in accordance with the regulations of the Italian Ministry of Health and the European Communities Council (86/609/EEC) directives.

Microarray analyses

Whole-genome microarray analysis of MSCs from differently aged mice was performed using the NimbleGen Gene Expression system. Briefly, total RNA was isolated from samples using the Qiagen RNeasy kit (Qiagen), following the manufacturer's instructions. RNA was used for cDNA synthesis, followed by labeling of the cDNA with Cy3. The labeled cDNA samples were hybridized to the *Mus musculus* 12×135K Array (Roche NimbleGen), which represents 44,170 mouse genes. The single color NimbleGen arrays were scanned using a GenePix 4400A Microarray Scanner. The data were extracted from scanned images using NimbleScan software, and the Robust Multichip Average (RMA) algorithm was used to generate gene expression values. Hybridization, scanning and normalization of the data were performed as a service by the Functional Genomic Center of the University of Verona (Verona, Italy). Whole-genome microarray of shIRF7 12-month-old MSCs was performed as service by the UTSW Genomics Sequencing & Microarray Core Facility (Dallas, TX, USA) on an Affymetrix platform (Clariom S Mouse Array).

Western blotting

Immunoblots were performed according to standard procedures in RIPA buffer (150 mM NaCl, 10 mM Tris pH 7.5, 1% NP40, 1% deoxycholate and 0.1% SDS) supplemented with phosphatase and protease inhibitors (Sigma-Aldrich). Samples were resolved on Tris-glycine 4–20% gradient SDS–PAGE gels (BIO-RAD), blotted on Protran 0.2 µm membrane (Whatman), incubated with anti-IRF7 (EPR4718; 1:500; ab109255; Abcam), anti-β-actin (Abcam, ab6276; 1:1000) or anti-GAPDH (Covance, #MMS-580S; 1:1000) antibody and developed with ECL (Amersham).

Quantitative PCR

RNA was extracted using the Qiagen RNAeasy Plus mini kit. cDNA was generated by Superscript II (Invitrogen) and used with SYBR Green PCR master mix (Applied Biosystems) for real-time qPCR analysis. Assays were performed using an Applied Biosystems Step-One Real-Time PCR System. Primers used for qPCR amplification are detailed in Table S1.

Transmission electron microscopy

Samples were fixed using 2% glutaraldehyde in Sorensen buffer pH 7.4 for 2 h, post-fixed in 1% osmium tetroxide in an aqueous solution for 2 h, dehydrated in graded concentrations of acetone, embedded in Epon-Araldite (Società Italiana Chimici) and cut with an Ultracut E Ultra-microtome (Reichert, Wien, Austria). At the end of the dehydration process, samples were positioned in a multi-well grid for electron microscopy and observed using a TEM Morgagni 268D (FEI Philips). Quantification of mitochondrial size was performed using ImageJ software (NIH, Bethesda, MD) on the images taken at the same magnification from 20 randomly selected fields.

shRNA IRF7 lentiviral transduction

IRF7 was silenced in 12-month-old aged MSCs by lentiviral transduction. Four different shIRF7 shRNAs in the pLKO.1 vector were used, named #1 (Dharmacon; RMM3981-201795252), #2 (Dharmacon; RMM3981-201798737), #3 (Dharmacon; RMM3981-201788865) and #4 (Dharmacon; RMM3981-201789942). Recombinant lentiviruses were generated in 293T cells transfected using the second-generation packaging vectors psPAX2 (Addgene #12260) and pMD2.G (Addgene #12259) using Lentifectin transfection reagent (ABM Good). Stable shIRF7 cells were selected with 1 mg/ml puromycin. 12-month-old MSCs transduced with empty (Addgene #10878) or shRNA scramble pLKO.1 (Addgene #1864) vectors were used as controls.

Metabolomic analysis

Cells were trypsinized, washed with phosphate-buffered saline (PBS) solution and centrifuged. Supernatants were removed, and cells were resuspended in PBS. Aliquots containing 10^6 cells were used for the metabolite extraction. Metabolites were extracted using 760 µl of a precooled MeOH:water mixture (1:0.9, v/v). Extracts were vortexed until complete dissolution of the pellet, and 400 µl of ice-cold chloroform was added. Cell extracts were then homogenized with a cell disrupter at 30 Hz for 10 min, then centrifuged at 2200 ***g*** for 5 min at 4°C. After layer separation, the polar and the nonpolar fractions were transferred to new precooled tubes. The aliquots were then evaporated to dryness using a nitrogen flow and stored at −80°C until analysis. Hexadecanoic acid as internal standard was added to the dried extract. The samples were first oximated by addition of 30 µl methoxyamine hydrochloride solution in pyridine (20 mg/ml), mixed in a vortex mixer and subsequently shaken for 90 min at 30°C. Afterwards, 30 µl of N,O-Bis(trimethylsilyl)trifluoroacetamide (BSTFA) with 1% trimethylchlorosilane (TMCS) was added, and the

derivatization was performed at 70°C for 60 min prior to gas chromatography–time of flight mass spectrometry (GC–TOF/MS) analysis. An alkane standard mixture (C8–C20; Merck KGaA) was added as internal standard.

GC–TOF/MS was performed using an Agilent 7890B GC (Agilent Technologies, USA) and Pegasus (BT) TOF/MS system (Leco Corporation, USA) equipped with an Rxi-5ms column (30 m×0.25 mm×0.25 µm; RESTEK, USA), stationary phase 5% diphenyl–95% dimethyl polysiloxane. High-purity helium (99.999%) was used as the carrier gas at a flow rate of 1.20 ml/min^{-1}. Samples were injected in splitless mode at 250°C. The chromatographic conditions were: initial temperature 70°C, 2 min isothermal, 6°C/min up to 160°C, 10°C/min up to 240°C, 20°C/min up to 300°C, 6 min isothermal. MS parameters: electron impact ionization source temperature (EI, 70 eV) was set at 250°C; scan range 40/630 *m/z*, with an extraction frequency of 30 kHz. The chromatograms were acquired in TIC (total ion current) mode. Mass spectral assignment was performed using the ChromaTOF BT software (Leco Corporation, USA) by matching with NIST MS Search 2.2. Libraries implemented with the MoNa Fiehns Libraries. Statistical and pathway studies were carried out using the MetaboAnalyst 4.0 tool (www.metaboanalyst.ca/).

Mitochondrial respiration

To analyze mitochondrial respiration in MSCs (including those transfected with either control or shIRF7 vectors) we used an Oxygraph-2K (Oroboros Instruments, Innsbruck). Instrumental and chemical background fluxes were opportunely calibrated as a function of oxygen concentration using DatLab software (Oroboros Instruments, Innsbruck). All the measures were performed comparing 12-month-old control and 12-month-old shIRF7 cells in parallel in the same experiment. Mitochondrial respiration was evaluated both in intact and permeabilized cells in different respiratory states (ROUTINE, LEAK, OXPHOS and ET) (Calabria et al., 2019; Erich, 2020).

Intact cells

Cells resuspended in DMEM (250,000 cells/ml) were analyzed applying a coupling control protocol (Pesta and Gnaiger, 2012) to determine the rate of oxygen consumption in the various respiratory states: ROUTINE (R), LEAK respiration (L), electron transfer capacity (ET) and residual oxygen consumption (ROX) (Pesta and Gnaiger, 2012). After stabilization of the rate of oxygen consumption in the ROUTINE state, respiration was supported with addition of pyruvate and malate (5 mM and 2 mM, respectively; Sigma-Aldrich), and the ATP-synthase inhibitor oligomycin (Omy; 2 µg/ml; Sigma-Aldrich) was added to obtain a measure of LEAK respiration. After this step followed the titration of CCCP (Sigma-Aldrich, #C-2759) to obtain maximum oxygen flux (ET capacity). Finally, rotenone (Rot) and antimycin A (Ama) were added to specifically inhibit complex I and complex III, respectively, in order to obtain the ROX.

Permeabilized cells

The respiration of permeabilized cells was determined using a modified substrate–uncoupler–inhibitor titration (SUIT) protocol (Pesta and Gnaiger, 2012). To investigate the contribution of different mitochondrial complexes (I–IV) to respiratory capacity, cells were permeabilized with the mild detergent digitonin (12 µg/10^{-6} cells; Sigma-Aldrich), this procedure allows specific substrates and adenylates to enter the cells and reach mitochondria. The optimal concentration of digitonin was evaluated in preliminary experiments as that suitable to achieve full permeabilization of cells allowing the access of substrates and ADP to mitochondria without compromising mitochondrial function. To evaluate the contribute of fatty acids to mitochondrial activity, octanoylcarnitine and malate (OM; 0.8 mM and 2 mM, respectively) were added in the ROUTINE state (R_{OM}). Following permeabilization with digitonin, the OXHPOS capacity (P_{OM}) was induced by adding ADP (5 mM; Sigma-Aldrich), and addition of glutamate (G; 10 mM) was used to determine complex I activity (P_{OMG}). To also activate complex II in OXPHOS, succinate (S) was added (P_{OMGS}; 10 mM succinate; Sigma-Aldrich). The presence of all these substrates (OMGS) allows detection of the respiratory activity of linked complex I, ETF and complex II. The contribution of complexes III and IV to respiratory activity is always present, although they were not stimulated by the addition of specific substrates.

To analyze the electron transfer system (ET_{OMGS}) capacity, stepwise titration with the uncoupler CCCP (0.5 µM steps; Sigma-Aldrich) was performed. Rot and Ama (2 and 2.5 µM, respectively; Sigma-Aldrich) were added to inhibit complex I (ET_S) and III, determining the ROX. Raw data were analyzed using the DatLab 6 Program (Oroboros Instruments).

Competing interests

The authors declare no competing or financial interests.

Author contributions

Conceptualization: A.N., A.F., A.S., F.S., M.K., M.G.; Methodology: A.N., I.S., D.P., E.C., D.B., S.M., M.M., A.F., S.V., E.M., M.G.; Software: A.B.; Validation: F.S., E.M., M.G.; Formal analysis: E.C., M.K., M.G.; Investigation: A.N., I.S., D.P., D.B., S.M., M.M., A.F., S.V., M.G.; Resources: A.N., I.S., D.P., A.B.; Data curation: A.N., I.S., D.P., E.C., M.M., A.B., M.K., M.G.; Writing - original draft: M.G.; Writing - review & editing: A.N., A.S., F.S., M.K., M.G.; Visualization: A.N., I.S., E.C., M.G.; Supervision: M.G.; Funding acquisition: A.S., M.G.

Funding

This research was funded by the Ministero dell'Istruzione, dell'Università e della Ricerca Progetti di Ricerca di Interesse Nazionale (PRIN; 2008YTNNBF_002).

Data availability

Raw and processed data of the microarray profiling of 1-month-old and 12-month-old MSCs are available at the NCBI Gene Expression Omnibus (GEO) repository (https://www.ncbi.nlm.nih.gov/geo/) under accession GSE25069. Raw and processed data of the microarray profiling of shIRF7 and control 12-month-old MSCs are available at GEO under accession GSE168533.

Peer review history

The peer review history is available online at https://journals.biologists.com/jcs/article-lookup/doi/10.1242/jcs.256230

References

Ashburner, M., Ball, C. A., Blake, J. A., Botstein, D., Butler, H., Cherry, J. M., Davis, A. P., Dolinski, K., Dwight, S. S., Eppig, J. T. et al. (2000). Gene ontology: tool for the unification of biology. The Gene Ontology Consortium. *Nat. Genet.* **25**, 25-29.

Baruch, K., Deczkowska, A., David, E., Castellano, J. M., Miller, O., Kertser, A., Berkutzki, T., Barnett-Itzhaki, Z., Bezalel, D., Wyss-Coray, T. et al. (2014). Aging. Aging-induced type I interferon response at the choroid plexus negatively affects brain function. *Science* **346**, 89-93.

Berry, D. C., Jiang, Y., Arpke, R. W., Close, E. L., Uchida, A., Reading, D., Berglund, E. D., Kyba, M. and Graff, J. M. (2017). Cellular aging contributes to failure of cold-induced beige adipocyte formation in old mice and humans. *Cell Metab.* **25**, 166-181. doi:10.1016/j.cmet.2016.10.023

Calabria, E., Scambi, I., Bonafede, R., Schiaffino, L., Peroni, D., Potrich, V., Capelli, C., Schena, F. and Mariotti, R. (2019). ASCs-exosomes recover coupling efficiency and mitochondrial membrane potential in an in vitro model of als. *Front Neurosci* **13**, 1070. doi:10.3389/fnins.2019.01070

Cardamone, M. D., Tanasa, B., Cederquist, C. T., Huang, J., Mahdaviani, K., Li, W., Rosenfeld, M. G., Liesa, M. and Perissi, V. (2018). Mitochondrial retrograde signaling in mammals is mediated by the transcriptional cofactor GPS2 via direct mitochondria-to-nucleus translocation. *Mol. Cell* **69**, 757-772.e7. doi:10.1016/j.molcel.2018.01.037

Chandel, N. S. (2015). Evolution of mitochondria as signaling organelles. *Cell Metab.* **22**, 204-206. doi:10.1016/j.cmet.2015.05.013

Channappanavar, R., Fehr, A. R., Vijay, R., Mack, M., Zhao, J., Meyerholz, D. K. and Perlman, S. (2016). Dysregulated type I interferon and inflammatory monocyte-macrophage responses cause lethal pneumonia in SARS-CoV-infected mice. *Cell Host Microbe* **19**, 181-193. doi:10.1016/j.chom.2016.01.007

Consortium, T. M. (2020). A single-cell transcriptomic atlas characterizes ageing tissues in the mouse. *Nature* **583**, 590-595. doi:10.1038/s41586-020-2496-1

D'Antona, G., Ragni, M., Cardile, A., Tedesco, L., Dossena, M., Bruttini, F., Caliaro, F., Corsetti, G., Bottinelli, R., Carruba, M. O. et al. (2010). Branched-chain amino acid supplementation promotes survival and supports cardiac and skeletal muscle mitochondrial biogenesis in middle-aged mice. *Cell Metab.* **12**, 362-372. doi:10.1016/j.cmet.2010.08.016

Darwin, C. (1859). *On the origin of species by means of natural selection, or, The preservation of favoured races in the struggle for life*. John Murray.

Davidson, S., Crotta, S., McCabe, T. M. and Wack, A. (2014). Pathogenic potential of interferon αβ in acute influenza infection. *Nat. Commun.* **5**, 3864. doi:10.1038/ncomms4864

Duran, M., Bruinvis, L., Ketting, D. and Wadman, S. K. (1978). Deranged isoleucine metabolism during ketotic attacks in patients with methylmalonic acidaemia. *J. Inherit. Metab. Dis.* **1**, 105-107. doi:10.1007/BF01805683
Erich, G. (2020). *Mitochondrial physiology*, vol. 1. Bioenerg Commun.
Fabregat, A., Sidiropoulos, K., Garapati, P., Gillespie, M., Hausmann, K., Haw, R., Jassal, B., Jupe, S., Korninger, F., McKay, S. et al. (2016). The reactome pathway knowledgebase. *Nucleic Acids Res.* **44**, D481-D487. doi:10.1093/nar/gkv1351
Felig, P., Marliss, E. and Cahill, G. F. (1969). Plasma amino acid levels and insulin secretion in obesity. *N. Engl. J. Med.* **281**, 811-816. doi:10.1056/NEJM196910092811503
Franceschi, C., Garagnani, P., Vitale, G., Capri, M. and Salvioli, S. (2017). Inflammaging and 'Garb-aging'. *Trends Endocrinol. Metab.* **28**, 199-212. doi:10.1016/j.tem.2016.09.005
Franceschi, C., Garagnani, P., Morsiani, C., Conte, M., Santoro, A., Grignolio, A., Monti, D., Capri, M. and Salvioli, S. (2018a). The continuum of aging and age-related diseases: common mechanisms but different rates. *Front Med* **5**, 61. doi:10.3389/fmed.2018.00061
Franceschi, C., Garagnani, P., Parini, P., Giuliani, C. and Santoro, A. (2018b). Inflammaging: a new immune-metabolic viewpoint for age-related diseases. *Nat Rev Endocrinol* **14**, 576-590. doi:10.1038/s41574-018-0059-4
Fumagalli, M., Sironi, M., Pozzoli, U., Ferrer-Admettlla, A., Ferrer-Admettla, A., Pattini, L. and Nielsen, R. (2011). Signatures of environmental genetic adaptation pinpoint pathogens as the main selective pressure through human evolution. *PLoS Genet.* **7**, e1002355. doi:10.1371/journal.pgen.1002355
Garaude, J., Acín-Pérez, R., Martínez-Cano, S., Enamorado, M., Ugolini, M., Nistal-Villán, E., Hervás-Stubbs, S., Pelegrín, P., Sander, L. E., Enríquez, J. A. et al. (2016). Mitochondrial respiratory-chain adaptations in macrophages contribute to antibacterial host defense. *Nat. Immunol.* **17**, 1037-1045. doi:10.1038/ni.3509
Gray, S., Wang, B., Orihuela, Y., Hong, E. G., Fisch, S., Haldar, S., Cline, G. W., Kim, J. K., Peroni, O. D., Kahn, B. B. et al. (2007). Regulation of gluconeogenesis by Krüppel-like factor 15. *Cell Metab.* **5**, 305-312. doi:10.1016/j.cmet.2007.03.002
Harding, H. P., Zhang, Y., Zeng, H., Novoa, I., Lu, P. D., Calfon, M., Sadri, N., Yun, C., Popko, B., Paules, R. et al. (2003). An integrated stress response regulates amino acid metabolism and resistance to oxidative stress. *Mol. Cell* **11**, 619-633. doi:10.1016/S1097-2765(03)00105-9
Honda, K. and Taniguchi, T. (2006). IRFs: master regulators of signalling by Toll-like receptors and cytosolic pattern-recognition receptors. *Nat. Rev. Immunol.* **6**, 644-658. doi:10.1038/nri1900
Honda, K., Yanai, H., Negishi, H., Asagiri, M., Sato, M., Mizutani, T., Shimada, N., Ohba, Y., Takaoka, A., Yoshida, N. et al. (2005). IRF-7 is the master regulator of type-I interferon-dependent immune responses. *Nature* **434**, 772-777. doi:10.1038/nature03464
Huffman, K. M., Shah, S. H., Stevens, R. D., Bain, J. R., Muehlbauer, M., Slentz, C. A., Tanner, C. J., Kuchibhatla, M., Houmard, J. A., Newgard, C. B. et al. (2009). Relationships between circulating metabolic intermediates and insulin action in overweight to obese, inactive men and women. *Diabetes Care* **32**, 1678-1683. doi:10.2337/dc08-2075
Jin, Z., Wei, W., Yang, M., Du, Y. and Wan, Y. (2014). Mitochondrial complex I activity suppresses inflammation and enhances bone resorption by shifting macrophage-osteoclast polarization. *Cell Metab.* **20**, 483-498. doi:10.1016/j.cmet.2014.07.011
Kim, J., Xu, M., Xo, R., Mates, A., Wilson, G. L., Pearsall, A. W. and Grishko, V. (2010). Mitochondrial DNA damage is involved in apoptosis caused by pro-inflammatory cytokines in human OA chondrocytes. *Osteoarthritis Cartilage* **18**, 424-432. doi:10.1016/j.joca.2009.09.008
Lerin, C., Goldfine, A. B., Boes, T., Liu, M., Kasif, S., Dreyfuss, J. M., De Sousa-Coelho, A. L., Daher, G., Manoli, I., Sysol, J. R. et al. (2016). Defects in muscle branched-chain amino acid oxidation contribute to impaired lipid metabolism. *Mol Metab* **5**, 926-936. doi:10.1016/j.molmet.2016.08.001
Levy, D. E., Marié, I., Smith, E. and Prakash, A. (2002). Enhancement and diversification of IFN induction by IRF-7-mediated positive feedback. *J. Interferon Cytokine Res.* **22**, 87-93. doi:10.1089/107999002753452692
Li, T., Zhang, Z., Kolwicz, S. C., Abell, L., Roe, N. D., Kim, M., Zhou, B., Cao, Y., Ritterhoff, J., Gu, H. et al. (2017). Defective branched-chain amino acid catabolism disrupts glucose metabolism and sensitizes the heart to ischemia-reperfusion injury. *Cell Metab.* **25**, 374-385. doi:10.1016/j.cmet.2016.11.005
López-Armada, M. J., Caramés, B., Martín, M. A., Cillero-Pastor, B., Lires-Dean, M., Fuentes-Boquete, I., Arenas, J. and Blanco, F. J. (2006). Mitochondrial activity is modulated by TNFalpha and IL-1beta in normal human chondrocyte cells. *Osteoarthritis Cartilage* **14**, 1011-1022. doi:10.1016/j.joca.2006.03.008
López-Otín, C., Blasco, M. A., Partridge, L., Serrano, M. and Kroemer, G. (2013). The hallmarks of aging. *Cell* **153**, 1194-1217. doi:10.1016/j.cell.2013.05.039
López-Otín, C., Galluzzi, L., Freije, J. M. P., Madeo, F. and Kroemer, G. (2016). Metabolic control of longevity. *Cell* **166**, 802-821. doi:10.1016/j.cell.2016.07.031
Lu, G., Ren, S., Korge, P., Choi, J., Dong, Y., Weiss, J., Koehler, C., Chen, J. N. and Wang, Y. (2007). A novel mitochondrial matrix serine/threonine protein phosphatase regulates the mitochondria permeability transition pore and is essential for cellular survival and development. *Genes Dev.* **21**, 784-796. doi:10.1101/gad.1499107
Lu, G., Sun, H., She, P., Youn, J. Y., Warburton, S., Ping, P., Vondriska, T. M., Cai, H., Lynch, C. J. and Wang, Y. (2009). Protein phosphatase 2Cm is a critical regulator of branched-chain amino acid catabolism in mice and cultured cells. *J. Clin. Invest.* **119**, 1678-1687. doi:10.1172/JCI38151
Lynch, C. J. and Adams, S. H. (2014). Branched-chain amino acids in metabolic signalling and insulin resistance. *Nat Rev Endocrinol* **10**, 723-736. doi:10.1038/nrendo.2014.171
MacMicking, J. D. (2012). Interferon-inducible effector mechanisms in cell-autonomous immunity. *Nat. Rev. Immunol.* **12**, 367-382. doi:10.1038/nri3210
Major, J., Crotta, S., Llorian, M., McCabe, T. M., Gad, H. H., Priestnall, S. L., Hartmann, R. and Wack, A. (2020). Type I and III interferons disrupt lung epithelial repair during recovery from viral infection. *Science*. **369**, 712-717. doi:10.1126/science.abc2061
Manaye, K. F., Mouton, P. R., Xu, G., Drew, A., Lei, D. L., Sharma, Y., Rebeck, G. W. and Turner, S. (2013). Age-related loss of noradrenergic neurons in the brains of triple transgenic mice. *Age* **35**, 139-147. doi:10.1007/s11357-011-9343-0
Mazière, C., Conte, M. A., Degonville, J., Ali, D. and Mazière, J. C. (1999). Cellular enrichment with polyunsaturated fatty acids induces an oxidative stress and activates the transcription factors AP1 and NFκB. *Biochem. Biophys. Res. Commun.* **265**, 116-122. doi:10.1006/bbrc.1999.1644
Milacic, M., Haw, R., Rothfels, K., Wu, G., Croft, D., Hermjakob, H., D'Eustachio, P. and Stein, L. (2012). Annotating cancer variants and anti-cancer therapeutics in reactome. *Cancers* **4**, 1180-1211. doi:10.3390/cancers4041180
Mori, M. A., Raghavan, P., Thomou, T., Boucher, J., Robida-Stubbs, S., Macotela, Y., Russell, S. J., Kirkland, J. L., Blackwell, T. K. and Kahn, C. R. (2012). Role of microRNA processing in adipose tissue in stress defense and longevity. *Cell Metab.* **16**, 336-347. doi:10.1016/j.cmet.2012.07.017
Mori, M. A., Thomou, T., Boucher, J., Lee, K. Y., Lallukka, S., Kim, J. K., Torriani, M., Yki-Järvinen, H., Grinspoon, S. K., Cypess, A. M. et al. (2014). Altered miRNA processing disrupts brown/white adipocyte determination and associates with lipodystrophy. *J. Clin. Invest.* **124**, 3339-3351. doi:10.1172/JCI73468
Newgard, C. B., An, J., Bain, J. R., Muehlbauer, M. J., Stevens, R. D., Lien, L. F., Haqq, A. M., Shah, S. H., Arlotto, M., Slentz, C. A. et al. (2009). A branched-chain amino acid-related metabolic signature that differentiates obese and lean humans and contributes to insulin resistance. *Cell Metab.* **9**, 311-326. doi:10.1016/j.cmet.2009.02.002
Pakos-Zebrucka, K., Koryga, I., Mnich, K., Ljujic, M., Samali, A. and Gorman, A. M. (2016). The integrated stress response. *EMBO Rep.* **17**, 1374-1395. doi:10.15252/embr.201642195
Papathanassiu, A. E., Ko, J. H., Imprialou, M., Bagnati, M., Srivastava, P. K., Vu, H. A., Cucchi, D., McAdoo, S. P., Ananieva, E. A., Mauro, C. et al. (2017). BCAT1 controls metabolic reprogramming in activated human macrophages and is associated with inflammatory diseases. *Nat. Commun.* **8**, 16040. doi:10.1038/ncomms16040
Peroni, D., Scambi, I., Pasini, A., Lisi, V., Bifari, F., Krampera, M., Rigotti, G., Sbarbati, A. and Galiè, M. (2008). Stem molecular signature of adipose-derived stromal cells. *Exp. Cell Res.* **314**, 603-615. doi:10.1016/j.yexcr.2007.10.007
Pesta, D. and Gnaiger, E. (2012). High-resolution respirometry: OXPHOS protocols for human cells and permeabilized fibers from small biopsies of human muscle. *Methods Mol. Biol.* **810**, 25-58. doi:10.1007/978-1-61779-382-0_3
Puthia, M., Ambite, I., Cafaro, C., Butler, D., Huang, Y., Lutay, N., Rydström, G., Gullstrand, B., Swaminathan, B., Nadeem, A. et al. (2016). IRF7 inhibition prevents destructive innate immunity-A target for nonantibiotic therapy of bacterial infections. *Sci Transl Med* **8**, 336ra59.
Quirós, P. M., Prado, M. A., Zamboni, N., D'Amico, D., Williams, R. W., Finley, D., Gygi, S. P. and Auwerx, J. (2017). Multi-omics analysis identifies ATF4 as a key regulator of the mitochondrial stress response in mammals. *J. Cell Biol.* **216**, 2027-2045. doi:10.1083/jcb.201702058
Randow, F., MacMicking, J. D. and James, L. C. (2013). Cellular self-defense: how cell-autonomous immunity protects against pathogens. *Science* **340**, 701-706. doi:10.1126/science.1233028
Rogers, N. H., Landa, A., Park, S. and Smith, R. G. (2012). Aging leads to a programmed loss of brown adipocytes in murine subcutaneous white adipose tissue. *Aging Cell* **11**, 1074-1083. doi:10.1111/acel.12010
Rosen, E. D. and Spiegelman, B. M. (2006). Adipocytes as regulators of energy balance and glucose homeostasis. *Nature* **444**, 847-853. doi:10.1038/nature05483
Rusinova, I., Forster, S., Yu, S., Kannan, A., Masse, M., Cumming, H., Chapman, R. and Hertzog, P. J. (2012). Interferome v2.0: an updated database of annotated interferon-regulated genes. *Nucleic Acids Res.* **41**, D1040-D1046. doi:10.1093/nar/gks1215
Schaum, N., Lehallier, B., Hahn, O., Pálovics, R., Hosseinzadeh, S., Lee, S. E., Sit, R., Lee, D. P., Losada, P. M., Zardeneta, M. E. et al. (2020). Ageing hallmarks exhibit organ-specific temporal signatures. *Nature* **583**, 596-602. doi:10.1038/s41586-020-2499-y

Schneider, W. M., Chevillotte, M. D. and Rice, C. M. (2014). Interferon-stimulated genes: a complex web of host defenses. *Annu. Rev. Immunol.* **32**, 513-545. doi:10.1146/annurev-immunol-032713-120231

Schoggins, J. W., Wilson, S. J., Panis, M., Murphy, M. Y., Jones, C. T., Bieniasz, P. and Rice, C. M. (2011). A diverse range of gene products are effectors of the type I interferon antiviral response. *Nature* **472**, 481-485. doi:10.1038/nature09907

Shavlakadze, T., Morris, M., Fang, J., Wang, S. X., Zhu, J., Zhou, W., Tse, H. W., Mondragon-Gonzalez, R., Roma, G. and Glass, D. J. (2019). Age-related gene expression signature in rats demonstrate early, late, and linear transcriptional changes from multiple tissues. *Cell Rep* **28**, 3263-3273.e3. doi:10.1016/j.celrep.2019.08.043

Shoji, H., Takao, K., Hattori, S. and Miyakawa, T. (2016). Age-related changes in behavior in C57BL/6J mice from young adulthood to middle age. *Mol Brain* **9**, 11. doi:10.1186/s13041-016-0191-9

Subramanian, A., Tamayo, P., Mootha, V. K., Mukherjee, S., Ebert, B. L., Gillette, M. A., Paulovich, A., Pomeroy, S. L., Golub, T. R., Lander, E. S. et al. (2005). Gene set enrichment analysis: a knowledge-based approach for interpreting genome-wide expression profiles. *Proc. Natl. Acad. Sci. U.S.A.* **102**, 15545-15550. doi:10.1073/pnas.0506580102

Suhm, T., Kaimal, J. M., Dawitz, H., Peselj, C., Masser, A. E., Hanzén, S., Ambrožič, M., Smialowska, A., Björck, M. L., Brzezinski, P. et al. (2018). Mitochondrial translation efficiency controls cytoplasmic protein homeostasis. *Cell Metab.* **27**, 1309-1322.e6. doi:10.1016/j.cmet.2018.04.011

Sun, H., Olson, K. C., Gao, C., Prosdocimo, D. A., Zhou, M., Wang, Z., Jeyaraj, D., Youn, J. Y., Ren, S., Liu, Y. et al. (2016a). Catabolic defect of branched-chain amino acids promotes heart failure. *Circulation* **133**, 2038-2049. doi:10.1161/CIRCULATIONAHA.115.020226

Sun, N., Youle, R. J. and Finkel, T. (2016b). The mitochondrial basis of aging. *Mol. Cell* **61**, 654-666. doi:10.1016/j.molcel.2016.01.028

Szklarczyk, D., Morris, J. H., Cook, H., Kuhn, M., Wyder, S., Simonovic, M., Santos, A., Doncheva, N. T., Roth, A., Bork, P. et al. (2017). The STRING database in 2017: quality-controlled protein-protein association networks, made broadly accessible. *Nucleic Acids Res.* **45**, D362-D368. doi:10.1093/nar/gkw937

Teijaro, J. R., Ng, C., Lee, A. M., Sullivan, B. M., Sheehan, K. C., Welch, M., Schreiber, R. D., de la Torre, J. C. and Oldstone, M. B. (2013). Persistent LCMV infection is controlled by blockade of type I interferon signaling. *Science* **340**, 207-211. doi:10.1126/science.1235214

The Gene Ontology Consortium (2017). Expansion of the gene ontology knowledgebase and resources. *Nucleic Acids Res.* **45**, D331-D338.

Timmons, J. A., Volmar, C. H., Crossland, H., Phillips, B. E., Sood, S., Janczura, K. J., Törmäkangas, T., Kujala, U. M., Kraus, W. E., Atherton, P. J. et al. (2019). Longevity-related molecular pathways are subject to midlife "switch" in humans. *Aging Cell* **18**, e12970. doi:10.1111/acel.12970

Turer, A. T., Stevens, R. D., Bain, J. R., Muehlbauer, M. J., van der Westhuizen, J., Mathew, J. P., Schwinn, D. A., Glower, D. D., Newgard, C. B. and Podgoreanu, M. V. (2009). Metabolomic profiling reveals distinct patterns of myocardial substrate use in humans with coronary artery disease or left ventricular dysfunction during surgical ischemia/reperfusion. *Circulation* **119**, 1736-1746. doi:10.1161/CIRCULATIONAHA.108.816116

van Horssen, J., van Schaik, P. and Witte, M. (2017). Inflammation and mitochondrial dysfunction: a vicious circle in neurodegenerative disorders?. *Neurosci. Lett.* **710**, 132931. doi:10.1016/j.neulet.2017.06.050

Vastrik, I., D'Eustachio, P., Schmidt, E., Joshi-Tope, G., Gopinath, G., Croft, D., de Bono, B., Gillespie, M., Jassal, B., Lewis, S. et al. (2007). Reactome: a knowledge base of biologic pathways and processes. *Genome Biol.* **8**, R39. doi:10.1186/gb-2007-8-3-r39

Walsh, D. and Mohr, I. (2011). Viral subversion of the host protein synthesis machinery. *Nat. Rev. Microbiol.* **9**, 860-875. doi:10.1038/nrmicro2655

Wathelet, M. G., Lin, C. H., Parekh, B. S., Ronco, L. V., Howley, P. M. and Maniatis, T. (1998). Virus infection induces the assembly of coordinately activated transcription factors on the IFN-beta enhancer in vivo. *Mol. Cell* **1**, 507-518. doi:10.1016/S1097-2765(00)80051-9

Wrobel, L., Topf, U., Bragoszewski, P., Wiese, S., Sztolsztener, M. E., Oeljeklaus, S., Varabyova, A., Lirski, M., Chroscicki, P., Mroczek, S. et al. (2015). Mistargeted mitochondrial proteins activate a proteostatic response in the cytosol. *Nature* **524**, 485-488. doi:10.1038/nature14951

Wu, D., Ren, Z., Pae, M., Guo, W., Cui, X., Merrill, A. H. and Meydani, S. N. (2007). Aging up-regulates expression of inflammatory mediators in mouse adipose tissue. *J. Immunol.* **179**, 4829-4839. doi:10.4049/jimmunol.179.7.4829

Wu, L. E., Gomes, A. P. and Sinclair, D. A. (2014). Geroncogenesis: metabolic changes during aging as a driver of tumorigenesis. *Cancer Cell* **25**, 12-19. doi:10.1016/j.ccr.2013.12.005

Xie, X., Lu, J., Kulbokas, E. J., Golub, T. R., Mootha, V., Lindblad-Toh, K., Lander, E. S. and Kellis, M. (2005). Systematic discovery of regulatory motifs in human promoters and 3′ UTRs by comparison of several mammals. *Nature* **434**, 338-345. doi:10.1038/nature03441

Zhang, Q., Raoof, M., Chen, Y., Sumi, Y., Sursal, T., Junger, W., Brohi, K., Itagaki, K. and Hauser, C. J. (2010). Circulating mitochondrial DAMPs cause inflammatory responses to injury. *Nature* **464**, 104-107. doi:10.1038/nature08780

Zid, B. M., Rogers, A. N., Katewa, S. D., Vargas, M. A., Kolipinski, M. C., Lu, T. A., Benzer, S. and Kapahi, P. (2009). 4E-BP extends lifespan upon dietary restriction by enhancing mitochondrial activity in Drosophila. *Cell* **139**, 149-160. doi:10.1016/j.cell.2009.07.034